Supporting Information for

Alleviating excessive aggregation of non-fullerene acceptor by delaying and shortening the crystallization time to reduce the energy loss of ternary organic solar cells

Jiaqi Pan,[a,b] Jian Guan,[a,b] Zehao Wang,[a,b] Rui Zhang,[c] Yingying Fu,[a] Xinhong Yu,[a] Qiang Zhang[a] and Yanchun Han*[a,b]*

[a] *State Key Laboratory of Polymer Physics and Chemistry, Changchun Institute of Applied Chemistry, Chinese Academy of Sciences, Changchun 130022, P. R. China*
[b] *School of Applied Chemistry and Engineering, University of Science and Technology of China, Hefei 230026, P.R. China*
[c] *Department of Physics, Chemistry and Biology (IFM), Linköping University, Linköping, Sweden*

* To whom correspondence should be addressed:
E-mail: rui.zhang@liu.se (Rui Zhang) ; ychan@ciac.ac.cn (Yanchun Han)

Table of Contents

10. UV-vis Absorption Spectroscopy

Figure S13. (a) The normalized absorption spectra of PM6 film with different PYIT weight ratios. (b) The normalized absorption spectra of Y6 film with different PYIT weight ratios.

11. Film-Depth-Dependent Light Absorption Spectroscopy

12. GIWAXS Measurement

Figure S14. (a) 2D GIWAXS images. (b) GIWAXS intensity profiles of the neat films along the out-of-plane direction.

Figure S15. (a) 2D GIWAXS images. (b) GIWAXS intensity profiles of the blend films along the out-of-plane direction.

Figure S16. Normalized in-situ absorption intensity at the wavelength of 625 nm and 800 nm as a function of film formation time for PM6:Y6 and PM6:Y6+15wt%PYIT blends.

13. Femtosecond time-resolved transient absorption spectra (FLAS)

14. Auxiliary Table

Table S1. Energy level of acceptor changes corresponding to different PYIT weight ratios.

Table S2. Photovoltaic performance parameters of the OSCs based on PM6:Y6+15 wt% PY-IT with different CN additive volume ratio, under the illumination of AM 1.5G, 100 mW cm^{-2}.

Table S3. Photovoltaic performance parameters of the OSCs based on PM6:Y6+20 wt% PY-IT with different CN additive volume ratio, under the illumination of AM 1.5G, 100 mW cm^{-2}.

Table S4. Detailed photovoltaic parameters for the devices based on BHJ PM6:Y6+PYIT active layers .

Table S5. Key parameters calculated from the Jph-Veff curves.

Table S6. Detailed Eloss parameters of the optimal binary and ternary devices.

Table S7. Summary of contact angles (θ), surface tensions (γ) and Flory-Huggins interaction parameters (χ) for PM6, Y6 and PYIT films.

Table S8. The absorption peak change of PM6 after adding different contents of PYIT.

Table S9. Changes in absorption peak positions of Y6 after the addition of PYIT with different contents.

Table S10. GIWAXS Parameters of the out-of-plane (010) peak in neat and blend films.

Table S11. GIWAXS Parameters of the out-of-plane (100) peak in neat and blend films.

Table S12. The fitted time of exciton dynamics for active layers.

1. Device Characterization

The current density–voltage (J-V) characteristics were tested under AM 1.5G irradiation (100 mW cm^{-2}) using a Keithley 2400 source meter. A QE-R 3011 was employed to give EQE data. EQE_{EL} measurements were performed by applying external voltage/current sources through the devices (REPS, Enlitech). The FTPS-EQE measurement was carried out on an Enlitech FTPS PECT-600 instrument.

2. Cyclic voltammetry (CV)

Cyclic voltammetry curves were carried out on a CHI660A electro-chemical work station. Using a standard three-electrode system, in thie system, a glassy-carbon electrode, Ag/AgCl and platinum wire were used as a working electrode, counter electrode and reference electrode, respectivelly. The samples were spin coated on the working electrode to be tested. The electrodes were dipeed in a 0.1 mol L^{-1} tetrabutylammonium hexafluorophosphate (Bu4NPF6) acetonitrile solution, with a scanning rate of 50 mV s^{-1}. Using ferrocene/ferrocenyl couple (Fc/Fc+) to calibrate. The highest occupied molecular orbital (HOMO) and lowest unoccupied molecular orbital (LUMO) energy levels can be calculated according to the oxidation potential (E_{OX}), reduction potential (E_{red}) and $E_{FC/FC+}$ with the equations (1-1) and (1-2):

$$E_{HOMO} = -(E_{OX} + 4.8 - E_{FC/FC+})eV \quad (1\text{-}1)$$

$$E_{LUMO} = -(E_{red} + 4.8 - E_{FC/FC+})eV \quad (1\text{-}2)$$

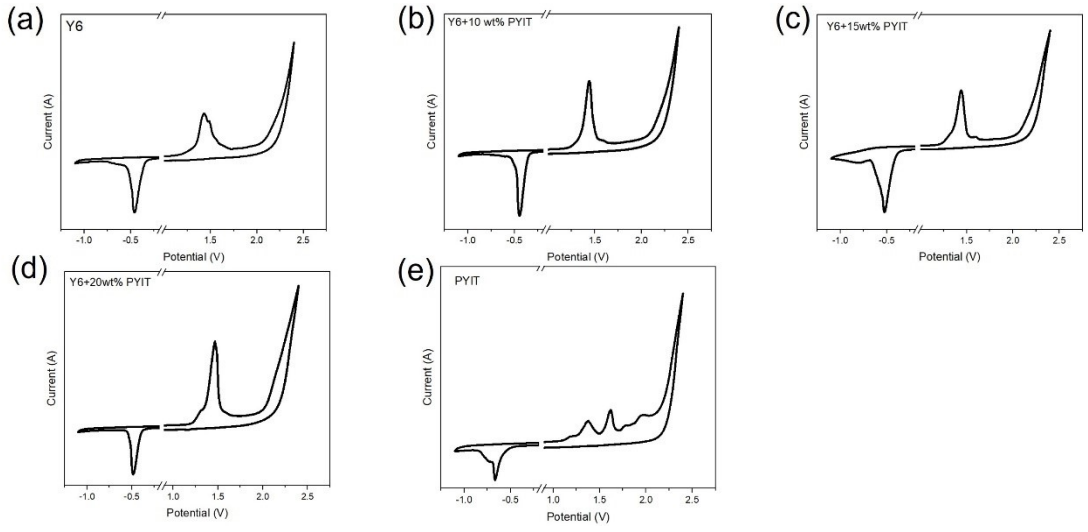

Figure S1. Cyclic voltammograms of the (a) Y6 film, (b) Y6+10wt%PYIT film, (c)

Y6+15wt%PYIT film, (d) Y6+20wt%PYIT film and (e) PYIT film.

3. Device performance:J-V and EQE Measurement

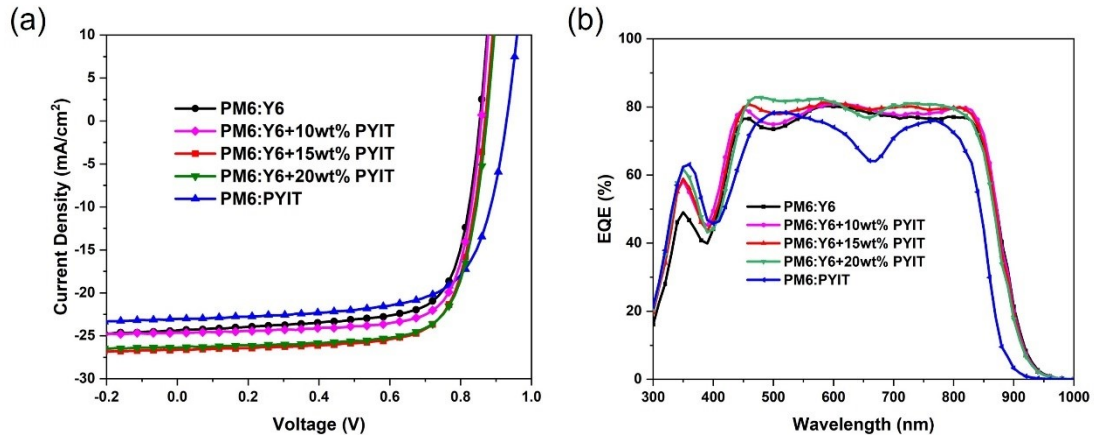

Figure S2. (a) *J-V* curves of the optimal binary and ternary OSCs with different polymer weight ratios under the illumination of AM 1.5G, 100 mW cm-2. (b) EQE spectra of optimal binary and ternary devices.

4. Stability Tests

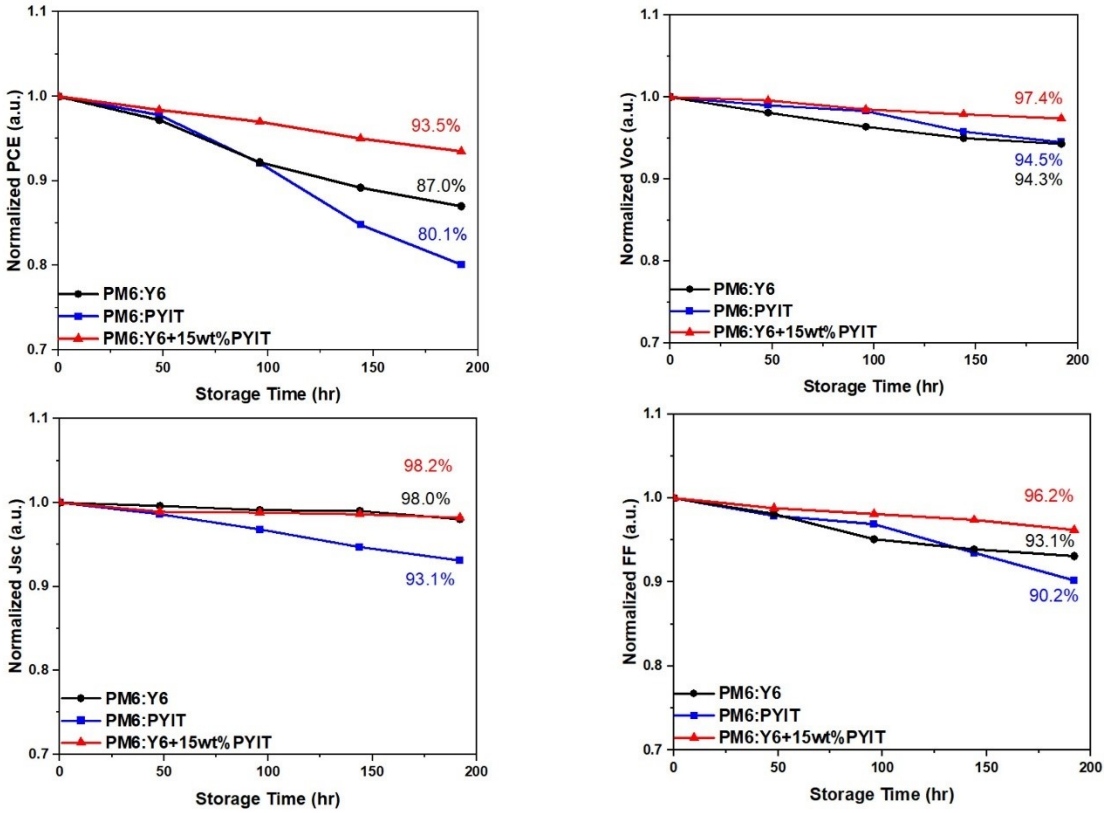

Figure S3. Storage stability in a nitrogen-filled glove of the un-encapsulated PM6:Y6 and PM6:Y6+PYIT devices.

5. SCLC Measurements

The electron-only and hole-only devices were prepared with the structure of ITO/ZnO/active layers/PDINN/Ag and ITO/PEDOT:PSS/active layers/MoO_3/Ag, respectively. The electron and hole mobilities were evaluated from space-charge-limited-current (SCLC) method, according to the Mott–Gurney square law: $J = 9\varepsilon_r\varepsilon_0\mu V^2/8d^3$,where J represents the current density in dark state, ε_r is the dielectric constant of used materials (for organic materials the ε_r parameter is assumed to be 3), ε_0 is the permittivity of free space (8.85×10^{-14}F/cm), V is the applied voltage and d is active layer thickness.

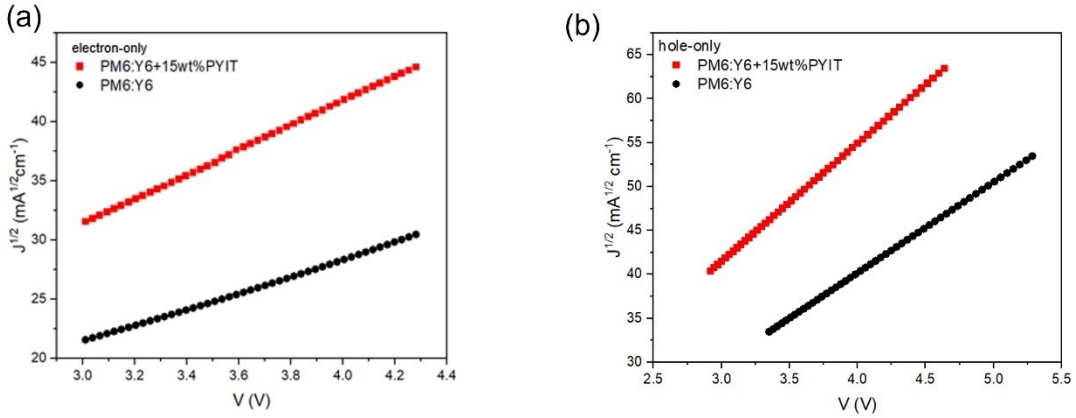

Figure S4. $J^{1/2}$~V (V = Vappl-Vbi-Vs) characteristics of the (a) electron-only and (b) hole-only devices.

6. Testing for Eg , Highly Sensitive EQE and EL spectra.

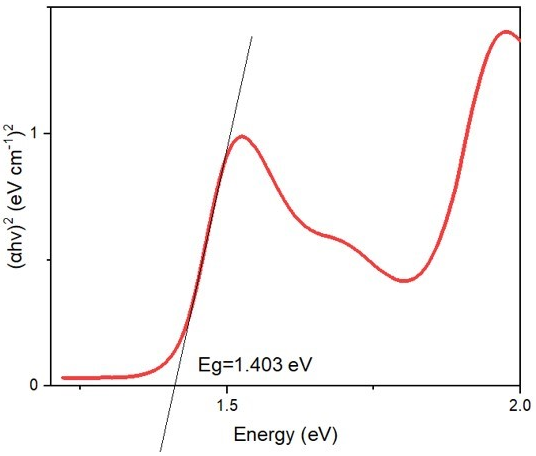

Figure S5. Absorbance spectra to determin the E_g.

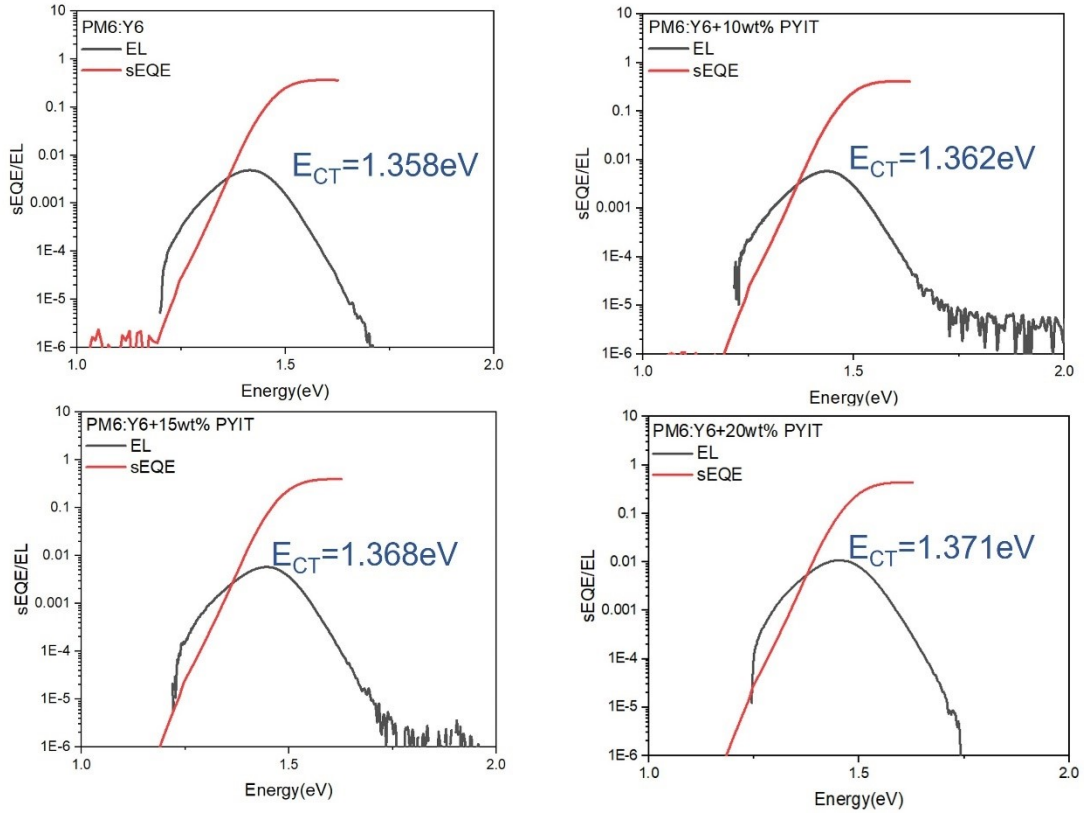

Figure S6. EL and s-EQE spectra of the binary and ternary devices.

7. Electroluminescence Quantum Efficiency

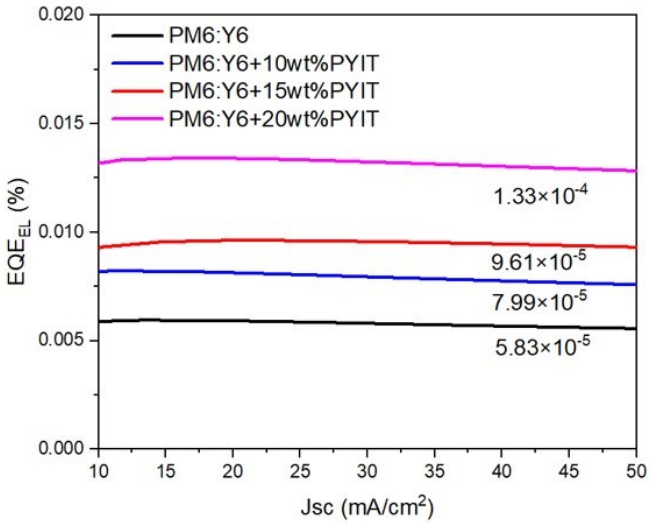

Figure S7. EQE_{EL} curves of the optimal binary and ternary devices.

8. Surface energy characterization

The contact angle measurements of films were measured with a contact angle goniometer (KRUSS GmbH Germany DO3021 Mk1). The surface energy of PM6, Y6 and PYIT films were calculated according to the Owens-Wendt method (1-3) and (1-4):

$\gamma_s = \gamma_s^p + \gamma_s^d$ (1-3)

$(1 + cos\Theta_l)\gamma_l = 2(\sqrt{\gamma_l^d \gamma_s^d} + \sqrt{\gamma_l^p \gamma_s^p})$ (1-4)

In the equations, γ_s, $\gamma_s^p$and γ_s^d are the total surface energy, polar component and dispersive component of surface energy, respecively; γ_l, γ_l^p and γ_l^d are the total surface energy, polar component and dispersive component of surface energy of the test liquid(water and diiodomethane), respectively. $\gamma_{diiodomethane} =$ 50.8 mJ/m^2, $\gamma_{water} =$ 72.8 mJ/m^2, $\gamma_{water}^{d} =$ 21.8 mJ/m^2, $\gamma_{water}^{p} =$ 51 mJ/m^2.

The miscibility of two materials canbe reflected by the Flory–Huggins interaction parameter (χ), which is obtained via using the equation (1-5):

$\chi_{D,A} = \kappa(\sqrt{\gamma_D} - \sqrt{\gamma_A})_2$ (1-5)

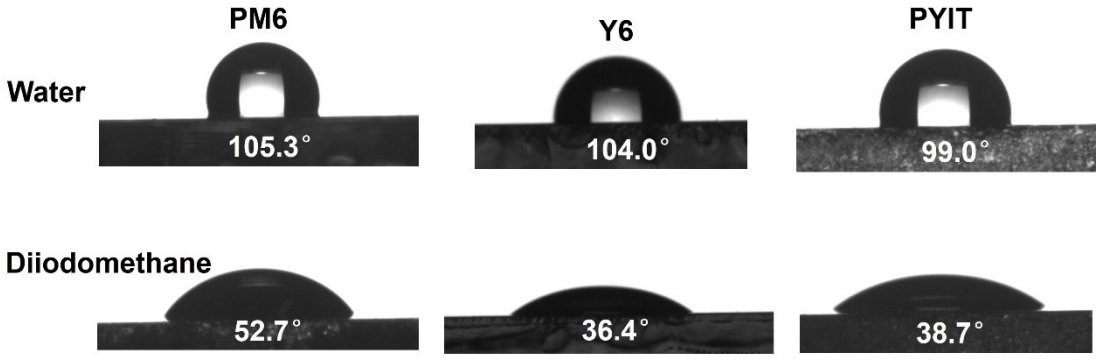

Figure S8. Contact angle images of neat PM6, Y6 and PYIT films.

9. AFM and TEM Measurement

The morphology of the active layers was tested by AFM using a Agilent 5500 AFM in a tapping-mode. In order to maintain the same conditions as the devices, the active layers were spin coated on PEDOT:PSS-coated ITO substrates. The TEM images of active layers were collected by a JEOL JEM-1400 transmission electron microscope operated at 120 kV. The active layers were spin coated onto the PEDOT:PSS-coated ITO substrates, then used the deionized water to dissolve the PEDOT:PSS layer and picked up the active layers using copper grids.

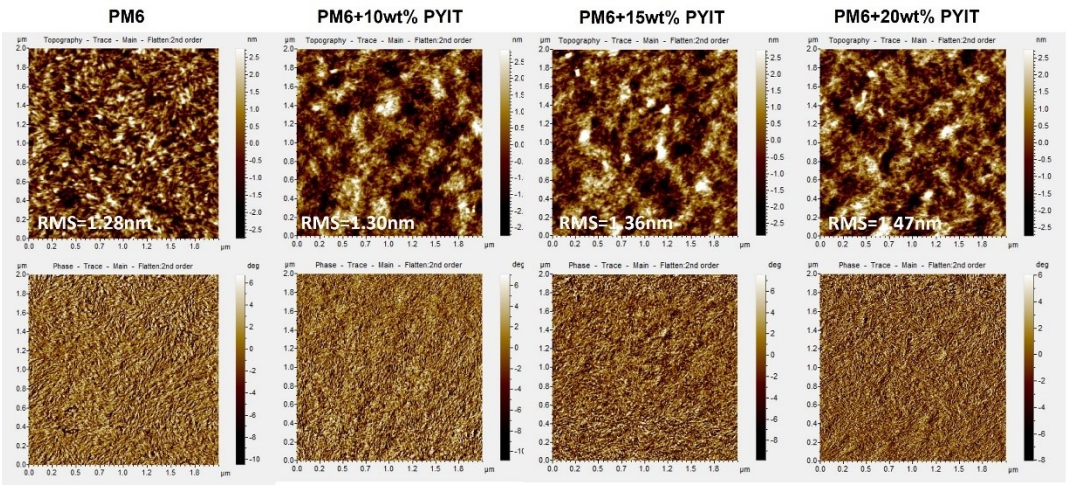

Figure S9. AFM height/phase images of the PM6 films with different PYIT weight ratios.

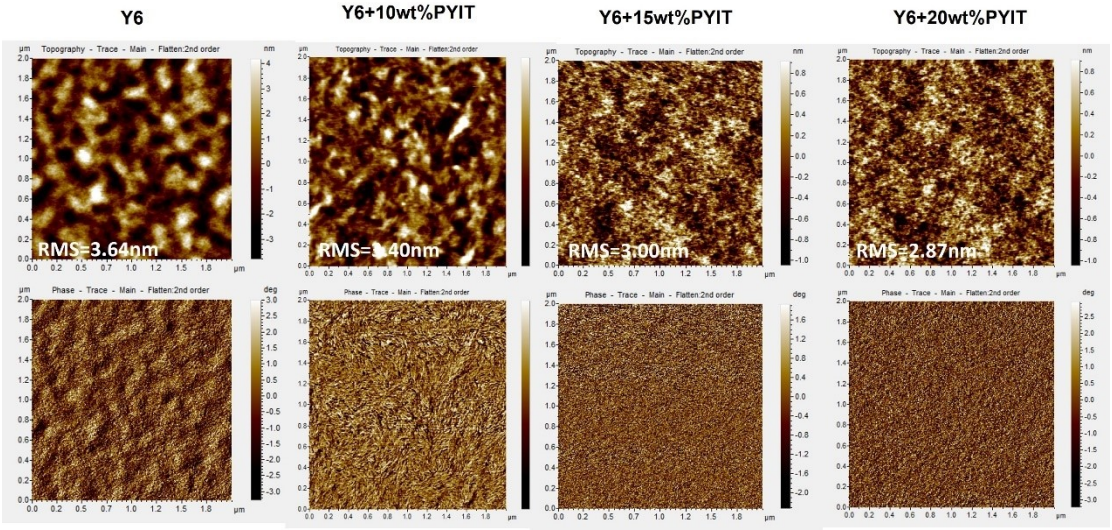

Figure S10. AFM height/phase images of the Y6 films with different PYIT weight ratios.

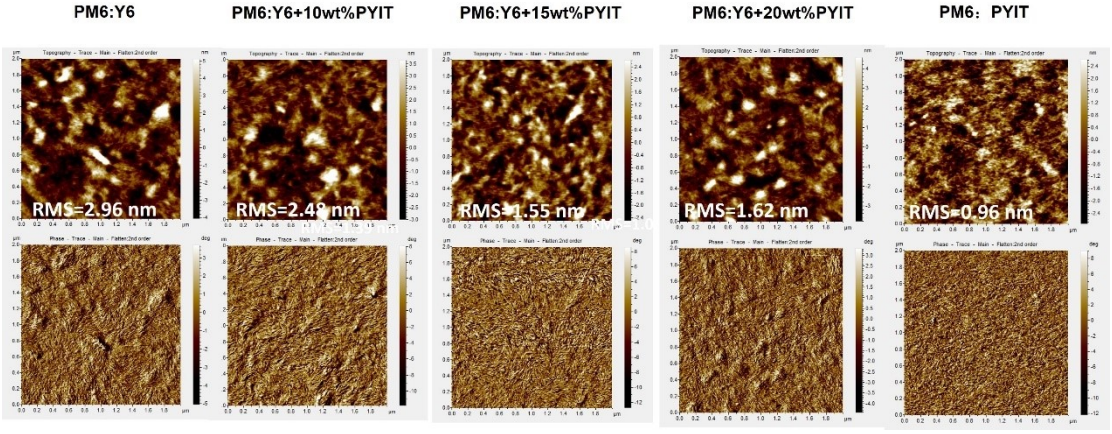

Figure S11. AFM height/phase images of the PM6:Y6, PM6:Y6+PYIT and PM6:PYIT films.

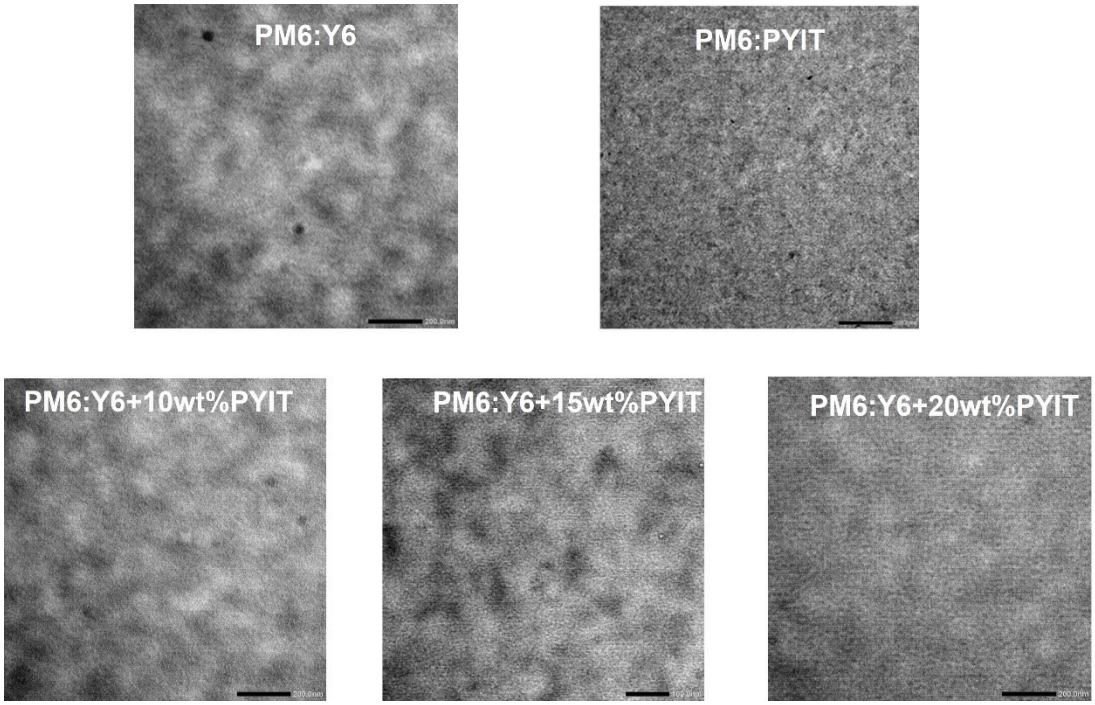

Figure S12. TEM images of binary and ternary films.

10. UV-vis Absorption Spectroscopy

The ultraviolet-visible (UV-vis) absorption spectra of films and in situ UV−vis absorption spectra were tested with a Lambda 750 spectrum .

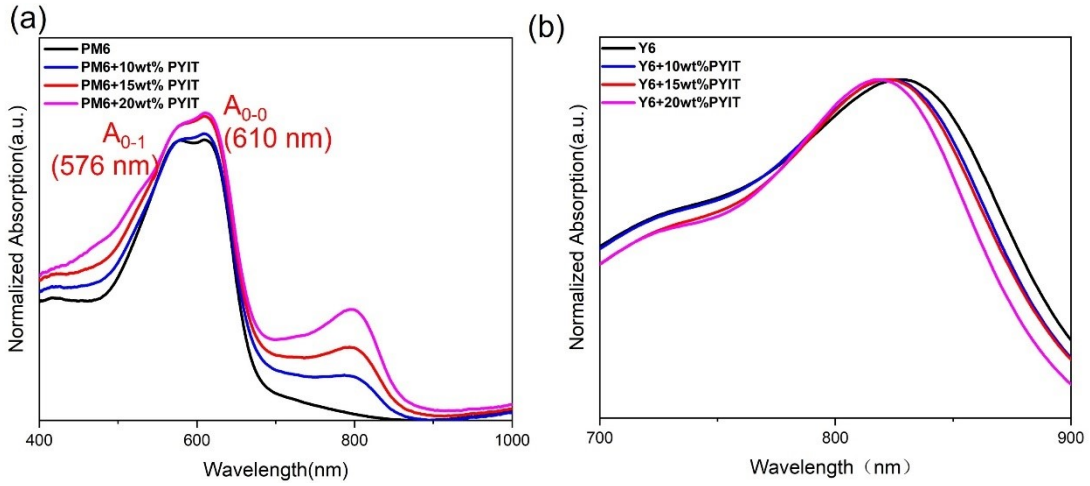

Figure S13. (a) The normalized absorption spectra of PM6 film with different PYIT weight ratios. (b) The normalized absorption spectra of Y6 film with different PYIT weight ratios.

11. Film-Depth-Dependent Light Absorption Spectroscopy

For film-depth-dependent light-absorption spectroscopy, the active layers were placed in an etching machine (Diener ZEPTO Plasma). It was found that a 20 nm thick thin

film can be etched in about 30s. After each etching, the light absorption characteristics of the active layer to different wavelengths of light were characterized by UV-vis absorption spectroscopy. The process was repeated to obtain UV-visible absorption spectra at different etching depths. In-situ UV-vis can be used to characterize the film formation kinetics process from solution state to thin film state. The time interval between each spectral acquisition is 0.05s, starting from the solution state and stopping after the film state stabilized.

12. Grazing incidence wide-angle X-ray scattering (GIWAXS)

The GIWAXS data were obtained at 1W1A Diffuse X-ray Scattering Station, Beijing Synchrotron Radiation Facility (BSRF-1W1A).

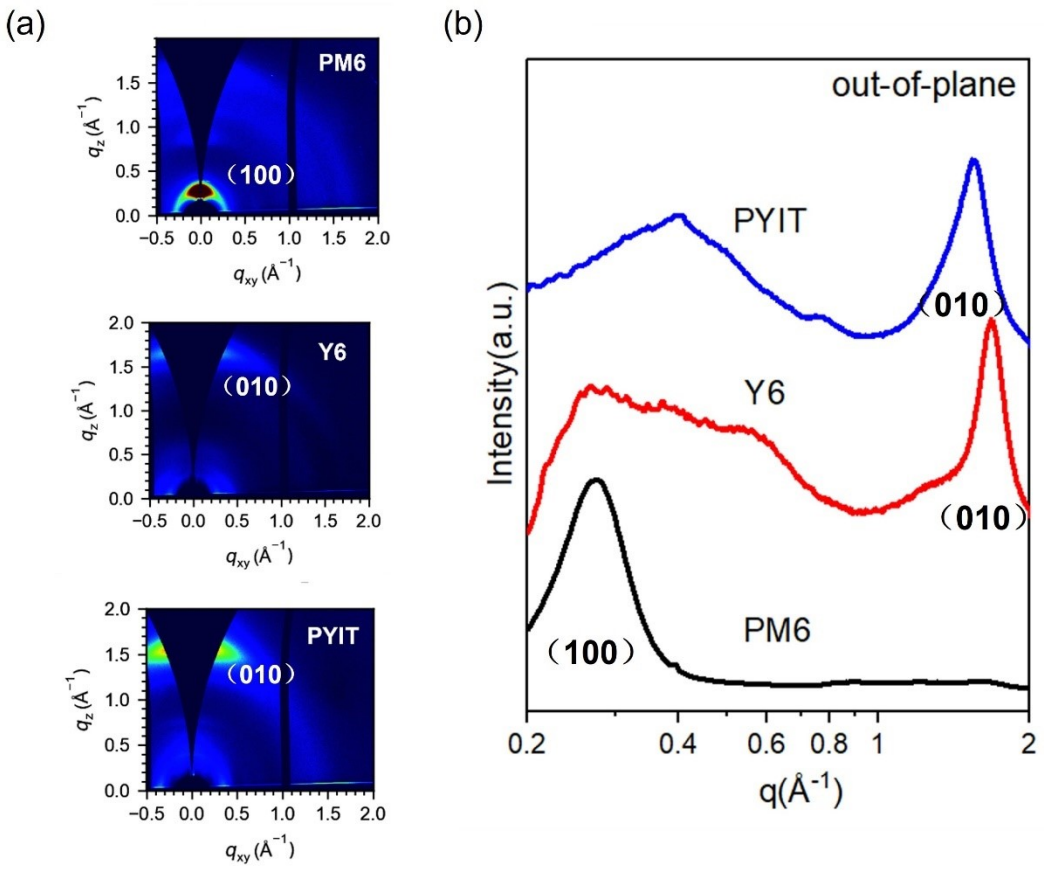

Figure S14. (a) 2D GIWAXS images. (b) GIWAXS intensity profiles of the neat films along the out-of-plane direction.

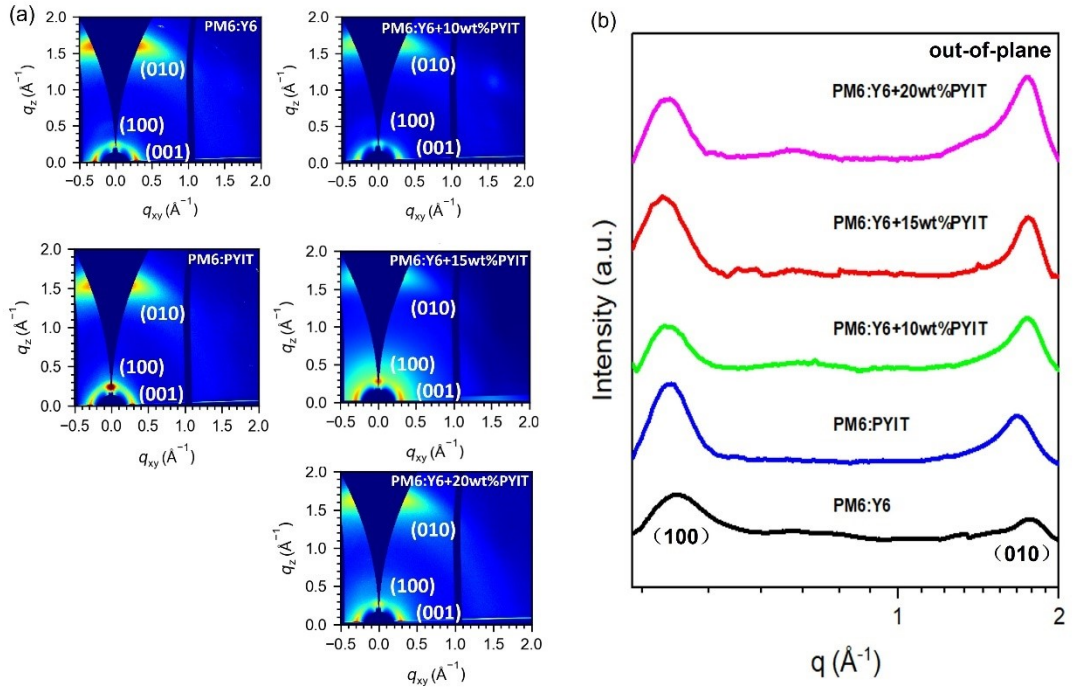

Figure S15. (a) 2D GIWAXS images. (b) GIWAXS intensity profiles of the blend films along the out-of-plane direction.

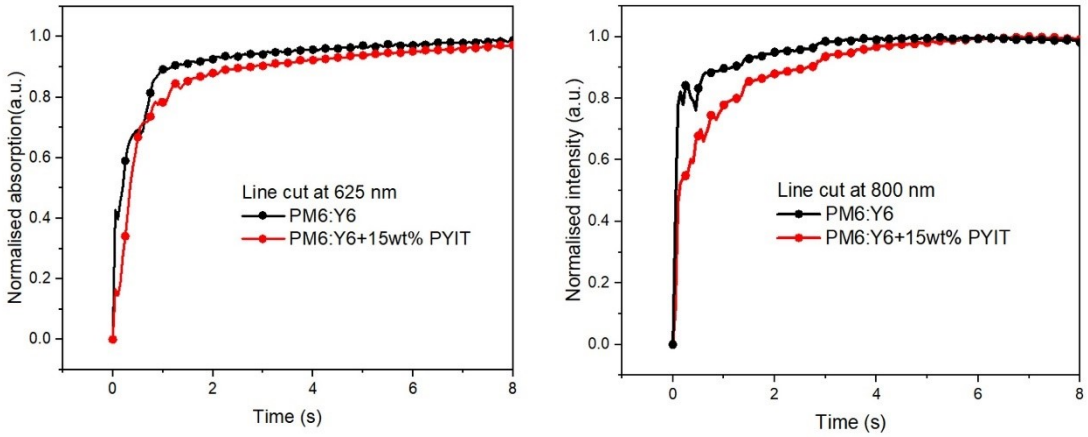

Figure S16. Normalized in-situ absorption intensity at the wavelength of 625 nm and 800 nm as a function of film formation time for PM6:Y6 and PM6:Y6+15wt%PYIT blends.

13. Femtosecond time-resolved transient absorption spectra (FLAS)

The femtosecond time-resolved transient absorption spectra measurement was performed using a femtosecond pump−probe system. The examples were made on ultrasonic-cleaned quartz slices (only active layers, no interface layers), then transfered the substrates into the glove box and seal it with quartz slices. The intensity of excitation used for testing was 20 nJ pulse^{-1}, the excitation wavelength was 800nm(only the

acceptor in active layer was excited).

14. Auxiliary Table

Table S1. Energy level of acceptor changes corresponding to different PYIT weight ratios.

Acceptor	LUMO(eV)	HOMO(eV)
Y6	-4.13	-5.80
Y6+10wt%PYIT	-4.11	-5.78
Y6+15wt%PYIT	-4.08	-5.69
Y6+20wt%PYIT	-4.06	-5.66
PYIT	-3.95	-5.56

Table S2. Photovoltaic performance parameters of the OSCs based on PM6:Y6+15 wt% PY-IT with different CN additive volume ratio, under the illumination of AM 1.5G, 100 mW cm^{-2}.

CN (vol %)	J_{SC} (mA/cm^2)	V_{OC}(V)	FF(%)	PCE(%)
0.50%	25.61 (25.54±0.05)	0.865 (0.863±0.001)	72.81 (72.48±0.64)	16.14 (15.99±0.14)
0.75%	26.15 (25.97±0.14)	0.864 (0.862±0.002)	75.39 (75.28±0.23)	17.05 (16.86±0.12)
1.00%	Device surface whitening			

Table S3. Photovoltaic performance parameters of the OSCs based on PM6:Y6+20 wt% PY-IT with different CN additive volume ratio, under the illumination of AM 1.5G, 100 mW cm^{-2}.

CN (vol %)	J_{SC}(mA/cm^2)	V_{OC}(V)	FF(%)	PCE(%)
0.50%	25.71 (25.65±0.05)	0.868 (0.865±0.002)	72.44 (72.44±0.36)	16.17 (16.16±0.01)

0.75%	26.37 (26.32±0.17)	0.873 (0.873±0.003)	73.87 (73.67±0.15)	17.02 (16.92±0.12)
1.00%	23.99 （23.78±0.23）	0.858 (0.857±0.001)	77.22 (77.15±0.08)	15.89 (15.73±0.16)

Table S4. Detailed photovoltaic parameters for the devices based on BHJ PM6:Y6+PYIT active layers .

PY-IT（wt %）	J_{SC}(mA/cm^2)	J_{SC}^{cal}(mA/cm^2)	V_{OC}(V)	FF(%)	PCE(%)
0	25.09 (24.81±0.66)	24.05	0.844 (0.845±0.004)	72.70 (73.26±0.73)	15.40 (15.32±0.19)
10	25.18 (24.96±0.23)	24.34	0.854 (0.853±0.002)	74.47 (74.05±0.28)	16.02 (15.78±0.23)
15	26.15 (25.97±0.14)	25.10	0.864 (0.862±0.002)	75.39 (75.28±0.23)	17.05 (16.86±0.12)
20	26.37 (26.32±0.17)	25.16	0.873 (0.873±0.003)	73.87 (73.67±0.15)	17.02 (16.92±0.12)
100	22.35 (21.98±0.33)	21.60	0.939 (0.937±0.002)	71.17 (71.15±0.15)	14.94 (14.65±0.28)

Table S5. Key parameters calculated from the Jph-Veff curves.

Device	J_{sat} (mA cm^{-2})	J_{SC}* (mA cm^{-2})	J_{max}& (mA cm^{-2})	N_{diss}	N_{coll}
PM6:Y6	25.45	24.71	22.65	97.09%	88.99%
PM6:Y6+15wt%PYIT	25.80	25.62	23.95	99.30%	92.83%

Table S6. Detailed Eloss parameters of the optimal binary and ternary devices.

Device	E_g(eV)	V_{OC}(V)	E_{loss}(ev)	E_{CT}(eV)	$\triangle E_{CT}$(ev)	$\triangle E_r$(eV)	$\triangle E_{nr}$(eV)	EQE_{EL}

PM6:Y6	1.403	0.844	0.559	1.358	0.045	0.270	0.244	5.83E-5
PM6:Y6+10wt%PYIT	1.403	0.854	0.549	1.362	0.041	0.273	0.235	7.99E-5
PM6:Y6+15wt%PYIT	1.403	0.864	0.539	1.368	0.035	0.273	0.231	9.61E-5
PM6:Y6+20wt%PYIT	1.403	0.873	0.530	1.371	0.032	0.275	0.223	1.33E-4

Table S7. Summary of contact angles (θ), surface tensions (γ) and Flory-Huggins interaction parameters (χ) for PM6, Y6 and PYIT films.

Sample	θ_{water}（°）	θ_{DIM}（°）	γ（mN/m）	χ^{D-A}	χ^{A1-A2}
PM6	105.3	52.7	32.75	/	/
Y6	104.0	36.4	41.49	0.516^{κ}	/
PYIT	99.0	38.7	40.28	0.389^{κ}	0.008^{κ}

Table S8. The absorption peak change of PM6 after adding different contents of PYIT.

	A_{0-1}	A_{0-0}	A_{0-0}/A_{0-1}
PM6	0.879	0.880	1.001
PM6+10wt% PYIT	0.886	0.899	1.015
PM6+15wt% PYIT	0.933	0.954	1.023
PM6+20wt% PYIT	0.937	0.965	1.030

Table S9. Changes in absorption peak positions of Y6 after the addition of PYIT with different contents.

	Peak position (nm)
Y6	827.39
Y6+10wt% PYIT	822.65
Y6+15wt% PYIT	821.34

Y6+20wt% PYIT	818.23

Table S10. GIWAXS Parameters of the out-of-plane (010) peak in neat and blend films.

Samples	q(Å^{-1})	d-spacing (Å)	FMHW(Å^{-1})	CCL(Å)
Y6	1.78	3.52	0.253	22.09
PYIT	1.65	3.80	0.367	15.22
PM6:Y6	1.75	3.58	0.220	25.40
PM6:Y6+10wt%PYIT	1.75	3.58	0.276	20.25
PM6:Y6+15wt%PYIT	1.75	3.58	0.285	19.61
PM6:Y6+20wt%PYIT	1.75	3.58	0.302	18.50
PM6:PYIT	1.67	3.76	0.308	18.15

Table S11. GIWAXS Parameters of the out-of-plane (100) peak in neat and blend films.

Samples	q(Å^{-1})	d-spacing (Å)	FMHW(Å^{-1})	CCL(Å)
PM6	0.37	16.97	0.101	55.34
PM6:Y6	0.36	17.44	0.081	69.00
PM6:Y6+10wt%PYIT	0.37	16.97	0.071	78.72
PM6:Y6+15wt%PYIT	0.37	16.97	0.070	79.84
PM6:Y6+20wt%PYIT	0.37	16.97	0.069	81.00
PM6:PYIT	0.38	16.53	0.074	75.53

Table S12. The fitted time of exciton dynamics for active layers.

Active layer	τ_1 （ps）	τ_2（ps）
PM6:Y6	0.37	5.27
PM6:Y6+15wt%PYIT	0.25	2.19